

# Polarization Talbot self-imaging with computer-generated, space-variant subwavelength dielectric gratings

Ze'ev Bomzon, Avi Niv, Gabriel Biener, Vladimir Kleiner, and Erez Hasman

Self-imaging of a periodic space-variant polarized field is demonstrated. The field is created by use of space-variant subwavelength dielectric gratings. Our observations include self-imaging of the fields at the Talbot planes as well as the translation of incident polarization variation into intensity modulation at certain planes. We demonstrate the formation of a one-dimensional nondiffracting beam with uniform intensity and a nontrivial polarization structure. © 2002 Optical Society of America

OCIS codes: 260.5430, 110.6760, 350.1370, 350.5500, 050.2770.

## 1. Introduction

The Talbot effect is a well-known interference phenomenon in which coherent illumination of a periodic structure gives rise to a series of self-images at well-defined planes.<sup>1</sup> This effect has many applications to fields such as wave-front sensing,<sup>2</sup> spectrometry,<sup>3</sup> and Talbot laser resonators.<sup>4</sup> Although most studies of the Talbot effect relate to waves for which the polarization is uniform, several contemporary papers have dealt with the Talbot effect in fields with space-variant (transversely inhomogeneous) polarization.<sup>5,6</sup> However, the experimental discussions were usually limited to simple binary anisotropic gratings or other discontinuous polarization distributions.

Recently we demonstrated the formation of continuous space-variant polarized fields by using computer-generated subwavelength dielectric gratings. By correctly controlling the local orientation and periodicity of the grating, one can achieve any desired space-variant polarization.<sup>7</sup> Furthermore, we showed that such polarization manipulations are necessarily accompanied by a space-variant phase manipulation of geometrical origin<sup>8</sup> that can be utilized for the formation of novel polarization-dependent phase elements, which we call Pancharatnam–Berry phase optical elements.<sup>9</sup>

In this paper we demonstrate a Talbot effect involving a unique type of polarization-diffraction grating that comprises a periodic space-variant wave plate for which the orientation of the fast axis varies linearly in the  $x$  direction. We show that for any incident polarization the resultant field undergoes self-imaging and fractional Talbot effects that involve polarization, intensity, and phase. We present a theoretical analysis of the phenomenon and experimentally demonstrate the effect, using a continuous space-variant subwavelength dielectric structure designed for CO<sub>2</sub> laser radiation at a wavelength of 10.6  $\mu\text{m}$ . Furthermore, we show that the Talbot effect for incident circular polarization yields a one-dimensional, nondiffracting beam that conserves its space-varying polarization and uniform intensity as it propagates.

## 2. Theory

Figure 1(a) is a schematic representation of a periodic space-variant wave plate for which the orientation of the fast axis,  $\theta$ , varies linearly in the  $x$  direction to form a polarization-diffraction grating with grating period  $d$ , which is larger than the wavelength of the incident wave,  $[\theta(x, y) = (\pi x/d)|_{\text{mod}\pi}]$ . When a plane wave with uniform polarization is incident upon such a space-varying wave plate the transmitted field will be periodic in both polarization and phase, and therefore we can expect this field to undergo Talbot self-imaging involving both polarization and phase at the appropriate planes.

Space-varying wave plates such as the one discussed above can be fabricated by use of subwavelength dielectric quasi-periodic structures. When the period of a subwavelength periodic structure is much smaller than the incident wavelength, only the zeroth order is a propagating order, and all other orders are evanes-

The authors are with the Optical Engineering Laboratory, Faculty of Mechanical Engineering, Technion—Israel Institute of Technology, Haifa 32000, Israel. E. Hasman's e-mail address is mehasman@tx.technion.ac.il.

Received 6 March 2002; revised manuscript received 20 May 2002.

0003-6935/02/255218-05\$15.00/0

© 2002 Optical Society of America

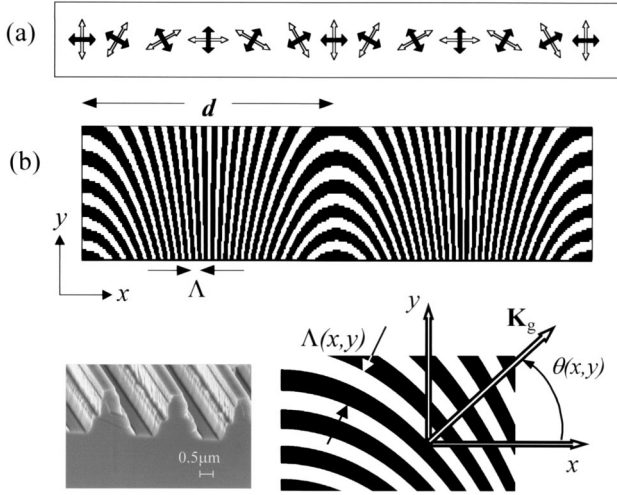


Fig. 1. (a) Space-varying polarization diffraction grating consisting of a periodic wave plate with a spatially rotating fast axis in the  $x$  direction. The period of the diffraction grating is  $d$ . Filled arrows show the local fast axis, whereas open arrows show the local slow axis. (b) Geometry of a space-variant subwavelength dielectric structure designed to act as the space-variant wave plate depicted in (a). Bottom left, scanning-electron microscope image of the subwavelength structure; bottom right, magnification of a region on the grating, demonstrating local subwavelength period  $\Lambda(x, y)$ , local grating orientation  $\theta(x, y)$ , and local subwavelength grating vector  $\mathbf{K}_g(x, y)$ .

cent. The subwavelength periodic structure behaves as a uniaxial crystal with the optical axes parallel and perpendicular to the subwavelength grooves. Therefore, by use of space-variant subwavelength quasi-periodic structures for which the local period and direction of the grooves vary continuously, space-variant wave plates can be designed. The local direction of the grooves controls the orientation of the wave plate, whereas the period, the depth, and the profile of the grooves control the retardation.<sup>7</sup>

Figure 1(b) demonstrates the geometry of a space-variant subwavelength structure designed to act as the wave plate illustrated in Fig. 1(a). The figure shows a continuous quasi-periodic subwavelength structure with local subwavelength period  $\Lambda(x, y)$  and with grooves oriented perpendicularly to the required fast axis. The local subwavelength periodicity gives the structure its birefringence, whereas the continuity of the subwavelength grooves ensures the continuity of the resultant field. Furthermore, we note the space-varying nature of  $\Lambda(x, y)$ . As we show in Section 3, the varied local subwavelength period is a necessary result of the requirement for continuity imposed on the subwavelength grooves.

It is convenient to describe space-variant subwavelength dielectric structures such as the one depicted in Fig. 1 by use of Jones calculus. In this representation a uniform subwavelength structure for which the grooves are oriented parallel to the  $y$  axis [ $\theta(x, y) = 0$ ] can be represented by the matrix

$$\mathbf{J} = \begin{bmatrix} 1 & 0 \\ 0 & e^{i\phi} \end{bmatrix}, \quad (1)$$

where  $\phi$  is the retardation of the subwavelength structure. If the orientation of the subwavelength grooves is space variant, i.e., different at each location, then the grating can be described by the space-dependent matrix

$$\mathbf{T}_C(x, y) = \mathbf{M}[\theta(x, y)]\mathbf{J}\mathbf{M}^{-1}[\theta(x, y)], \quad (2)$$

where  $\theta(x, y)$  is the local orientation of the grooves and

$$\mathbf{M}(\theta) = \begin{bmatrix} \cos \theta & -\sin \theta \\ \sin \theta & \cos \theta \end{bmatrix}$$

is a two-dimensional rotation matrix. For convenience we adopt Dirac bra-ket notation and convert  $\mathbf{T}_C(x, y)$  to a helicity base in which

$$|\mathbf{R}\rangle = \begin{pmatrix} 1 \\ 0 \end{pmatrix}, \quad |\mathbf{L}\rangle = \begin{pmatrix} 0 \\ 1 \end{pmatrix}$$

are the two-component unit vectors for right-hand and left-hand circularly polarized light, respectively. In this base the space-variant subwavelength structure is described by the matrix  $\mathbf{T}(x, y) = \mathbf{U}\mathbf{T}_C\mathbf{U}^{-1}$ , where

$$\mathbf{U} = \frac{1}{\sqrt{2}} \begin{bmatrix} 1 & i \\ 1 & -i \end{bmatrix}$$

is a unitary conversion matrix. Explicit calculation of  $\mathbf{T}(x, y)$  yields

$$\mathbf{T}(x, y) = \cos \frac{\phi}{2} \begin{bmatrix} 1 & 0 \\ 0 & 1 \end{bmatrix} - i \sin \frac{\phi}{2} \begin{bmatrix} 0 & \exp[-i2\theta(x, y)] \\ \exp[i2\theta(x, y)] & 0 \end{bmatrix}. \quad (3)$$

Consequently the Jones matrix that describes the element in Fig. 1 for which the local orientation of the subwavelength grooves is  $\theta(x, y) = \pi x/d|_{\text{mod}\pi}$  has the explicit form

$$\mathbf{T}(x, y) = \cos \frac{\phi}{2} \begin{bmatrix} 1 & 0 \\ 0 & 1 \end{bmatrix} - i \sin \frac{\phi}{2} \begin{bmatrix} 0 & \exp(-i2\pi x/d) \\ \exp(i2\pi x/d) & 0 \end{bmatrix}, \quad (4)$$

where we have assumed that the retardation  $\phi$  does not depend on  $\Lambda(x, y)$ . We previously showed that this assumption holds as long as  $\Lambda(x, y)$  does not exceed  $\lambda/n$ ,<sup>7</sup> where  $\lambda$  is the incident wavelength and  $n$  is the refractive index of the dielectric substrate upon which the structure is fabricated. Thus when a plane wave with arbitrary uniform polarization  $|\mathbf{E}_{\text{in}}\rangle$  is incident upon the element of Fig. 1 the resultant field is

$$\begin{aligned} &|\mathbf{E}_{\text{out}}(x, z = 0)\rangle \\ &= \cos \frac{\phi}{2} |\mathbf{E}_{\text{in}}\rangle - i \sin \frac{\phi}{2} [\eta_L|\mathbf{L}\rangle \exp(-i2\pi x/d) \\ &\quad + \eta_R|\mathbf{R}\rangle \exp(i2\pi x/d)], \end{aligned} \quad (5)$$

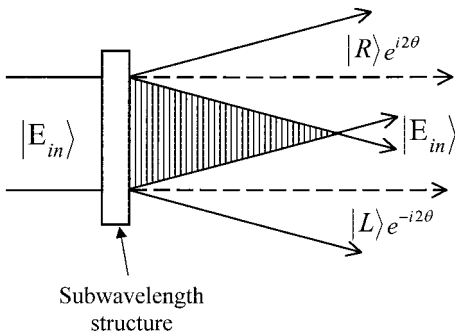


Fig. 2. Diffraction from the structure in Fig. 1. The Talbot effect occurs in the region where the diffracted orders overlap (the striped region).

where  $\eta_L = \langle \mathbf{E}_{in} | \mathbf{R} \rangle$  and  $\eta_R = \langle \mathbf{E}_{in} | \mathbf{L} \rangle$  and where  $\langle \alpha | \beta \rangle$  denotes an inner product. Figure 2 illustrates this result. When a uniformly polarized beam is incident upon the polarization grating, the resultant beam,  $|\mathbf{E}_{out}(x, z)\rangle$ , has three components: a zero order that maintains the original polarization and diffracted orders with  $|\mathbf{R}\rangle$  and  $|\mathbf{L}\rangle$  polarization. At each point the diffracted orders undergo phase modification equal to twice the angle of local orientation of the subwavelength grooves, and the phase of the  $|\mathbf{R}\rangle$  component is opposite in sign to the phase of the  $|\mathbf{L}\rangle$  component. Consequently the  $|\mathbf{R}\rangle$  and  $|\mathbf{L}\rangle$  polarized components are diffracted in opposite senses. The angle of diffraction is determined by the polarization grating period  $d$ . It should be noted that the phase modification of the diffracted orders results solely from local changes in polarization and is geometrical in nature.<sup>8,9</sup> We therefore denote it as the diffracted geometrical phase. Because the diffracted geometrical phases for both the  $|\mathbf{L}\rangle$  and the  $|\mathbf{R}\rangle$  diffracted orders have period  $d$ , we can expect Talbot self-imaging of each of these components at the same Talbot planes, resulting in a reconstruction of the field.

To prove that  $|\mathbf{E}_{out}\rangle$  undergoes self-imaging we calculate the propagation of each of the diffracted orders, using the Fresnel approximation,<sup>10</sup> to find that

$$\begin{aligned}
 |\mathbf{E}_{out}(x, z)\rangle = & \left\{ \cos \frac{\phi}{2} |\mathbf{E}_{in}\rangle \right. \\
 & - i \sin \frac{\phi}{2} \left[ \eta_L |\mathbf{L}\rangle \exp\left(-\frac{i2\pi x}{d} - \frac{i\pi\lambda z}{d^2}\right) \right. \\
 & \left. \left. + \eta_R |\mathbf{R}\rangle \exp\left(\frac{i2\pi x}{d} - \frac{i\pi\lambda z}{d^2}\right) \right] \right\} \\
 & \times \exp\left(\frac{i2\pi z}{\lambda}\right), \quad (6)
 \end{aligned}$$

from which we find that  $|\mathbf{E}_{out}(x, z = 0)\rangle = |\mathbf{E}_{out}(x, z = mZ_T)\rangle$ , where  $z = 0$  corresponds to the plane just after the grating,  $Z_T = 2d^2/\lambda$  is the Talbot distance, and  $m$  is an integer. The result of this calculation proves that  $|\mathbf{E}_{out}(x, z = 0)\rangle$  is reconstructed at the Talbot planes. Further analysis shows that  $|\mathbf{E}_{out}(x, z =$

$Z_T/2)\rangle = |\mathbf{E}_{out}(x + d/2, z = 0)\rangle$ . Thus, at half of the Talbot distance, the field is shifted in the  $x$  direction by half of a period relative to the field at  $z = 0$ , demonstrating a fractional Talbot effect. We can expect additional interesting effects at other fractional Talbot planes.

### 3. Realization and Experimental Results

To design a subwavelength structure with continuous subwavelength grooves, such as the one depicted in Fig. 1, we define a subwavelength grating vector  $\mathbf{K}_g = K_0(x, y)\{\cos[\theta(x, y)]\hat{x} + \sin[\theta(x, y)]\hat{y}\}$ .<sup>11</sup> Here  $\hat{x}$  and  $\hat{y}$  are unit vectors in the  $x$  and  $y$  directions,  $K_0 = 2\pi/\Lambda(x, y)$  is the spatial frequency of the local subwavelength structure, and  $\theta(x, y)$  is the space-variant direction of the vector, defined such that it is perpendicular to the subwavelength grooves at each point. The geometrical parameters of  $\mathbf{K}_g$  are shown in Fig. 1 (bottom right). To ensure the continuity of the subwavelength grooves we require that  $\nabla \times \mathbf{K}_g = 0$ , from which  $\Lambda(x, y)$  is determined. Once the equation has been solved, we calculate the grating function  $\phi_g$  (defined such that  $\nabla\phi_g = \mathbf{K}_g$ ) by integrating  $\mathbf{K}_g$  over an arbitrary path to yield  $\phi_g(x, y) = (2d/\Lambda_0)\sin(\pi x/d)\exp(-\pi y/d)$ , where  $\Lambda_0$  is the subwavelength period of the structure at  $y = 0$ . Figure 1(b) is a Lee-type binary structure<sup>11</sup> described by the grating function  $\phi_g$ .

We deposited the structure for CO<sub>2</sub> laser radiation with a wavelength of 10.6  $\mu\text{m}$  onto a GaAs wafer, with  $\Lambda_0 = 2 \mu\text{m}$  and  $d = 2.5 \text{ mm}$ . We formed the structure with a maximum local subwavelength period of  $\lambda/n = 3.24 \mu\text{m}$  ( $n = 3.27$  for GaAs). The length of the element in the  $x$  direction,  $l$ , was 30 mm; i.e.,  $l = 12d$ . First we fabricated a chrome mask of the structure, using high-resolution laser lithography. The pattern was then transferred by photolithography to a 500- $\mu\text{m}$ -thick GaAs wafer, after which we etched the structure by using electron cyclotron resonance with BCl<sub>3</sub> for 35 min. A scanning-electron microscope image of the subwavelength grooves is shown at the bottom left in Fig. 1. The structure yielded an effective space-variant wave plate with a measured local retardation of  $\phi = 65^\circ$ .

Following fabrication of the structure we illuminated it with linearly polarized light and measured the Stokes parameters<sup>12</sup> at various planes along the  $z$ -axis, using the four-measurement technique.<sup>13</sup> Figure 3 shows experimentally measured images of [Fig. 3(a)] the intensity measured at planes  $z = 0$ ,  $z = Z_T/4$ ,  $z = Z_T/2$ , and  $z = Z_T$  as well as [Fig. 3(b)] the measured and predicted Stokes parameters at these planes and [Fig. 3(c)] illustrations of the space-variant polarization ellipses at each plane. The experimental results agree with the predictions. At  $z = 0$  just after the grating, the polarization varies periodically and continuously in the  $x$  direction from linear polarization to nearly circular polarization, and the intensity is constant. This field is reconstructed at  $z = Z_T$ , thereby demonstrating the Talbot effect. At the plane  $z = Z_T/2$  we observe the shifted field as predicted from Eq. (6). A fractional Talbot

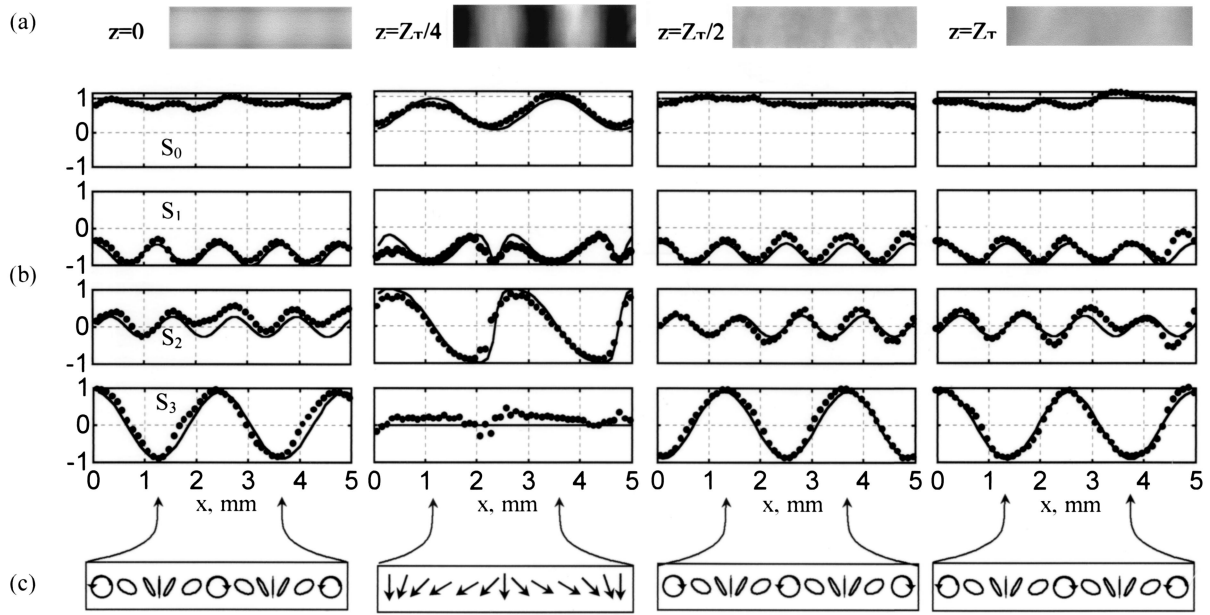


Fig. 3. (a) Measured intensity at planes  $z = 0$ ,  $z = Z_T/4$ ,  $z = Z_T/2$ , and  $z = Z_T$  for linear incident polarization. (b) Measured and predicted Stokes parameters and (c) illustration of the space-variant polarization ellipse at these planes.

effect is demonstrated at  $z = Z_T/4$ . At this plane a clear periodic variation in intensity is observable. Although the polarization at this plane is space varying, the ellipticity is zero and the beam is linearly polarized at all points. Further analysis of Eq. (6) shows that the visibility of the fringes at  $z = Z_T/4$  is equal to  $[1 - (S_3^{\text{in}})^2]^{1/2} \sin \phi$  ( $S_3^{\text{in}}$  is the third Stokes parameter of the incident beam), thereby providing a tool for characterization of the polarization of the incident beam.

A case of special interest occurs when  $|\mathbf{E}_{\text{in}}\rangle = |\mathbf{R}\rangle$ . Based on Eq. (5), the resultant beam for this case is

$$|\mathbf{E}_{\text{out}}\rangle = \cos \frac{\phi}{2} |\mathbf{R}\rangle - i \sin \frac{\phi}{2} |\mathbf{L}\rangle \exp(-i2\pi x/d). \quad (7)$$

Consequently  $|\mathbf{E}_{\text{out}}(x, z)\rangle$  comprises a zero order with  $|\mathbf{R}\rangle$  polarization and a single diffracted order with  $|\mathbf{L}\rangle$  polarization. Calculation of the Stokes parameters for this beam yields

$$\begin{aligned} S_0(x, z) &= 1, \\ S_1(x, z) &= -\sin \phi \sin(2\pi x/d + \pi\lambda z/d^2), \\ S_2(x, z) &= \sin \phi \cos(2\pi x/d + \pi\lambda z/d^2), \\ S_3 &= \cos \phi. \end{aligned} \quad (8)$$

The local ellipticity  $\chi$  and azimuthal angle  $\psi$  of the beam can be calculated from Eqs. (8) as<sup>13</sup>

$$\begin{aligned} \chi &= \frac{1}{2} \sin^{-1}(S_3/S_0) = \phi/2 + \pi/4, \\ \psi &= \frac{1}{2} \tan^{-1}(S_2/S_1) = \pi x/d + \pi\lambda z/2d^2 + \pi/4. \end{aligned} \quad (9)$$

The beam exhibits constant intensity and space-variant polarization in the entire object space. The ellipticity is constant and depends on the retardation of the wave plate, whereas the azimuthal angle varies

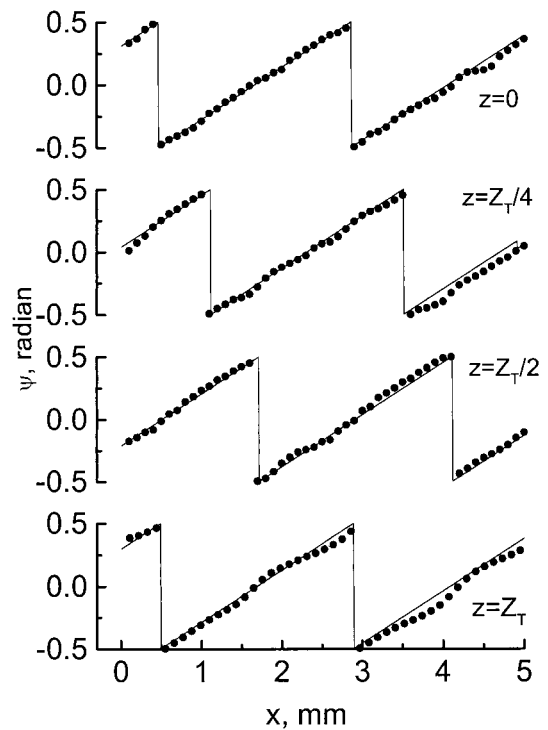


Fig. 4. Measured and predicted azimuthal angles when circular polarization is incident upon the polarization diffraction grating of Fig. 1 at planes  $z = 0$ ,  $z = Z_T/4$ ,  $z = Z_T/2$ , and  $z = Z_T$ .

linearly in the  $x$  direction. The polarization shifts in the  $x$  direction as the beam progresses, and the field is exactly reconstructed at  $z = Z_T$ . Figure 4 shows the experimental measurement of the azimuthal angle at various planes as well as the predicted results. The experiment is in good agreement with the theory, and we note the shifting polarization as the beam progresses.

The lateral shift in polarization can be canceled if we assume off-axis circularly polarized illumination of the grating at a small angle,  $\sin \alpha = \lambda/2d$ . Using Eqs. (5) and (6) and approximating  $\sin \alpha \approx \alpha$ , we find that the resultant field when  $\phi = \pi/2$  is

$$|\mathbf{E}_{\text{out}}(x,z)\rangle = [-\cos(2\pi x/d + \pi/4)\hat{x} + \sin(2\pi x/d + \pi/4)\hat{y}]\exp[i(2\pi z/\lambda + \pi/4)],$$

where  $\hat{x}$  and  $\hat{y}$  are Cartesian unit vectors transverse to the direction of propagation. The resultant beam has uniform intensity and a constant space-variant polarization that is retained throughout its propagation. The beam is essentially a one-dimensional vectorial nondiffracting beam that is analogous to a scalar nondiffracting cosine beam. However, the uniqueness of our solution lies in its space-varying polarization and uniform intensity, which make it better suited for applications such as metrology and three-dimensional scanning. Results that relate to the nondiffracting structure of the beam still hold when  $\phi \neq \pi/2$ .

To conclude, we have demonstrated Talbot effects that involve a space-variant polarized field by using subwavelength dielectric structures. We believe that these effects can be applied to the improvement of many existing Talbot-effect-based applications and point the way to the use of some novel ideas.

## References and Notes

1. See, for example, J. W. Goodman, *Introduction to Fourier Optics* (McGraw-Hill, New York, 1996), p. 87.

2. Ch. Siegel, F. Lowenthal, and J. E. Balmer, "A wavefront sensor based on the fractional Talbot effect," *Opt. Commun.* **194**, 265–275 (2001).
3. H. L. Kung, A. Bhatnagar, and D. A. B. Miller, "Transform spectrometer based on measuring the periodicity of Talbot self-images," *Opt. Lett.* **26**, 1645–1647 (2001).
4. M. Wraga, P. Glas, D. Fischer, M. Leitner, D. Vysotsky, and A. P. Napartovich, "Phase locking in a multicore fiber laser by means of a Talbot resonator," *Opt. Lett.* **25**, 1436–1438 (2000).
5. V. A. Arrizón, E. Tepchin, M. Ortiz-Gutierrez, and A. W. Lohmann, "Fresnel diffraction at  $1/4$  of the Talbot distance of an anisotropic grating," *Opt. Commun.* **127**, 171–175 (1996).
6. H. J. Rabal, W. D. Furlan, and E. E. Sicre, "Talbot interferometry with anisotropic gratings," *Opt. Commun.* **57**, 81–83 (1986).
7. Z. Bomzon, G. Biener, V. Kleiner, and E. Hasman, "Real time analysis of partially polarized light with a space-variant subwavelength dielectric grating," *Opt. Lett.* **27**, 285–287 (2002).
8. Z. Bomzon, V. Kleiner, and E. Hasman, "Pancharatnam–Berry phase in space-variant polarization-manipulations with subwavelength gratings," *Opt. Lett.* **26**, 1424–1426 (2001).
9. Z. Bomzon, G. Biener, V. Kleiner, and E. Hasman, "Space-variant Pancharatnam–Berry phase optical elements with computer-generated subwavelength gratings," *Opt. Lett.* **27**, 1141–1143 (2002).
10. The Fresnel approximation for the propagation of a scalar wave is defined as  $E(x, y, z) = \mathbf{F}^{-1}\mathbf{H}\mathbf{F}[E(x, y, z = 0)]$ , where  $E(x, y, z)$  is a scalar wave function,  $\mathbf{F}$  denotes a spatial Fourier transform,  $\mathbf{H}(f_x, z) = \exp(i2\pi z/\lambda)\exp(-i\pi\lambda z f_x^2)$  is the Fresnel transfer function, and  $f_x$  denotes spatial frequency. See, for example, Ref. 1.
11. Z. Bomzon, V. Kleiner, and E. Hasman, "Space-variant polarization state manipulation with computer-generated subwavelength metal-stripe gratings," *Opt. Commun.* **192**, 169–181 (2001).
12. Stokes parameters are used to define the polarization state. They are  $S_0 = |E_x|^2 + |E_y|^2$ ,  $S_1 = |E_x|^2 - |E_y|^2$ ,  $S_2 = E_x E_y^* + E_y E_x^*$ , and  $S_3 = i(E_x E_y^* - E_y E_x^*)$ , where  $E_x$  and  $E_y$  are the Cartesian components of the electromagnetic field.  $S_0$  is the intensity of the field, whereas  $S_1 \dots S_3$  define the polarization ellipse. See, for example, C. Brosseau, *Polarized Light, A Statistical Optics Approach* (Wiley, New York, 1998).
13. E. Collett, *Polarized Light* (Marcel Dekker, New York, 1993).